Data Fusion of Dual Foot-Mounted INS to Reduce the Systematic Heading Drift

Prateek G V, Girisha R and K.V.S. Hari
Statistical Signal Processing Lab
Department of ECE
Indian Institute of Science
Bangalore, India
Email: {prateekgv,girishar,hari}@ece.iisc.ernet.in

Peter Händel
Signal Processing Lab
ACCESS Linnaeus Center
KTH Royal Institute of Technology
Stockholm, Sweden
Email: ph@kth.se

***Abstract*—In this report, we investigate the problem of applying a range constraint in order to reduce the systematic heading drift in a foot-mounted inertial navigation system (INS) (motion-tracking). We make use of two foot-mounted INS, one on each foot, which are aided with zero-velocity detectors. A novel algorithm is proposed in order to reduce the systematic heading drift. The proposed algorithm is based on the idea that the separation between the two feet at any given instance must always lie within a sphere of radius equal to the maximum possible spatial separation between the two feet. A Kalman filter, getting one measurement update and two observation updates is used in this algorithm.**

***Keywords-Pedestrian Navigation System, Inertial Measurement Unit, Kalman Filter, Indoor Navigation, Systematic Heading Drift*.**

I. Introduction

A navigation system that is robust, with accurate positioning system with seemless indoor and outdoor coverage can increase the safety in emergency response and military operations [1]. The most commonly used navigation system is the GPS, that provides high accuracy in many scenarios. But, the main challenge is to create a navigation system that is sufficiently accurate in GPS denied environments. The key to achieving a system with good accuracy during indoor operations is to use appropriate positioning sensors. One such system that provides good accuracy is the OpenShoe [2], a real-time, embedded implementation of a foot-mounted, zero-velocity aided INS. The data presented in this article have been collected with OpenShoe units that were mounted below the heels. The orientation of the units is such that the y-axis points the forward direction or the direction of motion, z-axis points downwards and the x-axis points in medial direction. A detailed description of building an OpenShoe unit is presented in [2].

But as pointed out in [3], one of the drawbacks of the existing foot-mounted ZUPT-aided INS is the Systematic Heading Drift. The estimated trajectories drift away from the actual path as time progresses. Despite having a calibration phase before the walking starts, systematic heading drifts are still persistent. Another important observation to be made is that the drift obtained are symmetrical. These errors are large scale manifestations of modeling errors in the system. One possible way these errors can be mitigated is to use foot-mounted INS on both feet as suggested in [4] [5] [6] [7] such that the symmetrical modeling errors cancel out. As illustrated in Fig. 1, there is limit on the separation between the two feet which are equipped with zero-velocity aided INS.

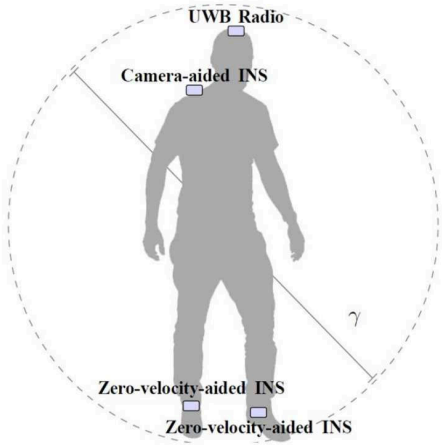

Figure 1: Illustration of the possible placements of the subsystem in a pedestrian navigation system and the maximum spatial separation γ between the subsystems. Image source: [4]

Notation: Bold lowercase represents a vector whereas bold uppercase represents a matrix. The superscript indicates the navigation system (in this case left or right foot-mounted zero-velocity aided INS). Alphabets mentioned as a subscript represent time-stamp and are always lowercase letters.

A brief explanation about the existing architecture, algorithm and trajectories obtained without applying range constraint on the spatial separation between two subsystems is studied in Section II. The experimental setup used for data collection is also presented in Secin II. A detailed description of the *proposed* algorithm and the pseudo code of the proposed algorithm is presented in Section III. Experiments and results obtained using the *proposed* and existing algorithms are presented in Section IV. Section V contains the Conclusions.

II. Without Range Constraint on the Spatial Separation Between Two Feet

In this section we look at the trajectories obtained without applying a range constraint on the spatial separation between the two feet equipped with foot-mounted IMU. We have tried to be consistent with the symbols used in this paper by following the notations used in [8]. Two OpenShoe units, one on each foot is integrated in the sole of the shoe with its USB end connected to the laptop. We use the GLRT algorithm [9] in order to detect the time epochs when the foot is stationary. The IMU transmits accelerometer and gyroscope readings in 3-axes at the rate of 819.2 samples/sec. The datasets obtained are made sure to be of the *same length* and are *synchronized*.

The state vector, $\delta\mathbf{x}_k^i \in \mathbb{R}^9$, is used in the Kalman filter and is defined as $\delta\mathbf{x}_k^i = [\delta\mathbf{p}_k^{i\,T}\delta\mathbf{v}_k^{i\,T}\boldsymbol{\delta\theta}_k^{i\,T}]^T$, where $\delta\mathbf{p}_k^i \in \mathbb{R}^3$ denotes the position error, $\delta\mathbf{v}_k^i \in \mathbb{R}^3$ denotes the velocity error, $\boldsymbol{\delta\theta}_k^i \in \mathbb{R}^3$ denotes the attitude error, i denotes the navigation system and $i \in \{l, r\}$ at k^{th} time instant where l and r represents the left and right foot navigation system respectively. The state space model is given by

$$\begin{aligned}\delta\mathbf{x}_{k+1}^i &= \begin{bmatrix}\mathbf{I}_3 & T_s\mathbf{I}_3 & \mathbf{0}_3\\ \mathbf{0}_3 & \mathbf{I}_3 & T_s[\mathbf{s}^{n_i}]_\times\\ \mathbf{0}_3 & \mathbf{0}_3 & \mathbf{I}_3\end{bmatrix}\delta\mathbf{x}_k^i + \begin{bmatrix}\mathbf{0}_3 & \mathbf{0}_3\\ \mathbf{R}_p^{n_i} & \mathbf{0}_3\\ \mathbf{0}_3 & \mathbf{R}_p^{n_i}\end{bmatrix}\mathbf{w}_k^{1i}\\ &= \mathbf{F}_k^i\delta\mathbf{x}_k^i + \mathbf{G}_k^i\mathbf{w}_k^{1i}. \qquad (1)\end{aligned}$$

Here $\mathbf{I}_3$ and $\mathbf{0}_3$ denote a three by three identity and zero matrices, respectively. $\mathbf{R}_p^{n_i}$ is the rotation matrix transforming a vector from platform to navigation coordinates [11] and $[\mathbf{s}^{n_i}]_\times$, the skew symmetric matrix representation of the specific force vector [11] $\mathbf{s}^{n_i} \in \mathbb{R}^3$. The process noise $\mathbf{w}_k^{1i} \in \mathbb{R}^6$ is assumed to be white and the covariance matrix is defined as

$$\begin{aligned}\mathbf{Q}_k^i &= \mathbb{E}\{\mathbf{w}_k^{1i}(\mathbf{w}_k^{1i})^T\}\\ &= \begin{bmatrix}\sigma_a^2\mathbf{I}_3 & \mathbf{0}_3\\ \mathbf{0}_3 & \sigma_\omega^2\mathbf{I}_3\end{bmatrix}. \qquad (2)\end{aligned}$$

Here $\sigma_a^2 \in \mathbb{R}^1$ and $\sigma_\omega^2 \in \mathbb{R}^1$ denote the variance of the measurement noise of the accelerometers and gyroscopes, respectively.

Further $\mathbf{y}_k^i$ denotes the observed velocity error and $\Delta_k^i \in \{0, 1\}$ is the indicator function that indicates the time instants during which the IMU is stationary. The vector, $\mathbf{x}_k^i \in \mathbb{R}^9$, is defined as $\mathbf{x}_k^i = [\mathbf{p}_k^{i\,T}\mathbf{v}_k^{i\,T}\boldsymbol{\theta}_k^{i\,T}]^T$, where $\mathbf{p}_k^i \in \mathbb{R}^3$ denotes the position in the spatial coordinates, $\mathbf{v}_k^i \in \mathbb{R}^3$ denotes the velocity, $\boldsymbol{\theta}_k^i \in \mathbb{R}^3$ denotes the attitude, i denotes the navigation system and $i \in \{l, r\}$ at k^{th} time instant. The observed velocity error is defined as follows

$$\begin{aligned}\mathbf{y}_k^i &= \Delta_k^i\left(\begin{bmatrix}\mathbf{0}_3 & \mathbf{I}_3 & \mathbf{0}_3\end{bmatrix}\mathbf{x}_k^i + \mathbf{w}_k^{2i}\right) \qquad (3)\\ &= \Delta_k^i\left(\mathbf{H}_k^i\mathbf{x}_k^i + \mathbf{w}_k^{2i}\right) \qquad (4)\end{aligned}$$

The process noise $\mathbf{w}_k^{2i} \in \mathbb{R}^3$ is assumed to be white and the covariance matrix is defined as

$$\begin{aligned}\mathbf{R}_k^i &= \mathbb{E}\{\mathbf{w}_k^{2i}(\mathbf{w}_k^{2i})^T\} \qquad (5)\\ &= \sigma_v^2\mathbf{I}_3 \qquad (6)\end{aligned}$$

Here $\sigma_v^2 \in \mathbb{R}^1$ denotes the variance of measurement noise. $\mathbf{P}_k^i$ is defined as the error covariance matrix of the ith navigation system where $i \in \{l, r\}$. Under the assumption that the system is stationary during the first 20 samples, the initial roll and pitch is calculated [11] from the 20 first accelerometer readings as follows

$$\begin{aligned}r_0^i &= \tan^{-1}\left(-\bar{f}_v^i, -\bar{f}_w^i\right) \qquad (7)\\ p_0^i &= \tan^{-1}\left(\bar{f}_u^i, \sqrt{\bar{f}_v^{i\,2} + \bar{f}_v^{i\,2}}\right) \qquad (8)\\ y_0^i &= 0^\circ \qquad (9)\end{aligned}$$

where $[r_0^i, p_0^i, y_0^i]^T$ are the initial roll, pitch and yaw angles and $[\bar{f}_u^i, \bar{f}_v^i, \bar{f}_w^i]^T$ are the mean values of the first 20 samples of the accelerometer readings of the ith navigation system. The initial velocity is assumed to be zero, the initial position coordinates are assumed to be $[0, 0, 0]^T$ and the initial heading for i^{th} navigation system where $i \in \{l, r\}$ is assumed to be 0°.

A. Data Collection

This experiment was conducted on the first floor of the Signal Processing Building, Department of ECE, Indian Institute of Science, Bangalore, India. The corridor of the signal processing lab is an inverted 'U' shaped path with sharp 90° turns. For our convenience purpose we denote the segments of the inverted 'U' path as 'AB', 'BC' and 'CD' as shown in Fig. 4. In the real world point 'A' is room 2.21, the point 'B' is room 2.15, the point 'C' is room 2.07 and point 'D' is room 2.01. We asked the user, a 25 year old male with height 1.73 m and a weight of 68 kg, to walk on leveled ground. The tiles in the corridor helped us to collect data precisely. Each tile is a square of length 2 feet $= 0.6096 \times 2$m. The parallel arms of the corridor are of 34 m in length (58 tiles) and the perpendicular arm is 23 m (39 tiles) in length (approximately). Several trajectories of different shapes such as a straight trajectory (walking along a single parallel arm of the 'U' path) or an 'L' shaped trajectory (one parallel arm and one perpendicular arm of the 'U' path) or an inverted 'U' shaped (complete corridor) trajectory are obtained starting from point 'A' or point 'D'. The data collection was done in a controlled manner, such that, during the calibration phase of the IMU, both the feet are touching the ground and are stationary. While walking, we placed our foot exactly in the middle of the tile and made sure that at any given instance of time, the separation between the two feet did not exceed 0.6096[m]. The total time taken to cover the U path trajectory is 1:33:23 mins with 0:33:10 mins for segment AB, 0:25:3 mins for segment BC and 0:35:10 min for segment CD.

Algorithm 1 Pseudo code for the algorithm *without* range constraint on the spatial separation of the two navigation systems i, j where $i, j \in \{l, r\}$ and $i \neq j$.

$k \leftarrow 0$
$\mathbf{P}_k^i, \mathbf{Q}_k^i, \mathbf{R}_k^i, \mathbf{H}_k^i \leftarrow$ **Process**{Initialize Filter}
$\mathbf{P}_k^j, \mathbf{Q}_k^j, \mathbf{R}_k^j, \mathbf{H}_k^j \leftarrow$ **Process**{Initialize Filter}
$\hat{\mathbf{x}}_k^i \leftarrow$ **Process**{Initial Navigation State}
$\hat{\mathbf{x}}_k^j \leftarrow$ **Process**{Initial Navigation State}
loop
  $k \leftarrow k + 1$
  $\hat{\mathbf{x}}_k^i \leftarrow$ **Process**{Navigation Equations}
  $\hat{\mathbf{x}}_k^j \leftarrow$ **Process**{Navigation Equations}
  $\mathbf{P}_k^i \leftarrow \mathbf{F}_k^i \mathbf{P}_{k-1}^i {\mathbf{F}_k^i}^T + \mathbf{G}_k^i \mathbf{Q}_k^i {\mathbf{G}_k^i}^T$
  $\mathbf{P}_k^j \leftarrow \mathbf{F}_k^j \mathbf{P}_{k-1}^j {\mathbf{F}_k^j}^T + \mathbf{G}_k^j \mathbf{Q}_k^j {\mathbf{G}_k^j}^T$
  for $s \in \{l, r\}$ **do**
    if $\mathbf{zupt}_k^s$ is **on then**
      $\mathbf{K}_k^s \leftarrow \mathbf{P}_k^s {\mathbf{H}_k^s}^T [\mathbf{H}_k^s \mathbf{P}_k^s {\mathbf{H}_k^s}^T + \mathbf{R}_k^s]^{-1}$
      $\delta \mathbf{x}_k^s \leftarrow -\mathbf{K}_k^s [\hat{\mathbf{x}}_k^s]_{4:6}$
      $\hat{\mathbf{x}}_k^s \leftarrow$ **Process**{Correct Navigation States}
      $\mathbf{P}_k^s \leftarrow [\mathbf{I} - \mathbf{K}_k^s \mathbf{H}_k^s] \mathbf{P}_k^s$
    end if
  end for
end loop

B. Observation

Even though both the IMUs were aligned in the same direction, but on different feet, the two trajectories take two different paths. None of the trajectories obtained from the left foot or right foot represent the actual path as shown in Fig. 4. Another important observation made is that, in certain cases both left and right feet trajectories lie in the same quadrant, but in other cases, they lie in the adjacent quadrants. Also, we understand that the initial heading value plays a *dominant* role while plotting a trajectory. We will study the importance of initial heading information in next sections.

III. Applying Range Constraint on the Spatial Separation Between Two Feet

In this section we propose a new algorithm to unify the trajectories obtained from two foot-mounted IMUs aligned in the same direction using an upper bound in the spatial region. In [10], the authors classify the gait cycle for runners and walkers into four phases, namely Push-off, Swing, Heel Strike and Stance for a single foot. The duration of the phases of the gait cycle for walkers shows that for more than 50% of the time the foot occupies Heel-strike and Stance phase. Fig. 2 shows a screen shot of the Stance phase or ZUPT occurrences using GLRT algorithm [9]. It can be observed, during walking, somewhere in between the push-off, swing and heel-strike phase of the left foot, the Stance phase for the right foot occurs and vice versa. The duration of the stance phase changes if the person walks faster or runs. From what we understand after carefully observing the motion of two feet is, the foot that is in stance phase helps the other foot generate momentum for its push-off and swing phase.

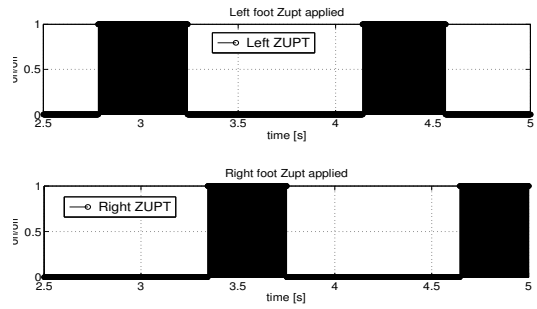

Figure 2: A snapshot of the ZUPTs occurrences for left and right foot from time instance 2.5[s] to 5[s] for a Straight Path trajectory using the GLRT algorithm [9].

Also, studying the motion of the feet of a person during walking or running, we notice that the separation between the two feet does not exceed a certain threshold value. In other words, when one foot is in its stance phase, the position of the foot that is in motion cannot exceed a threshold value, which we define as the maximum spatial bound. Let γ be the maximum possible separation between the two feet at any instance of time. When the two feet are stationary, with the help of zero-velocity instances, the error covariance can be minimized as seen in Algorithm 1. But it is during the motion of the foot, that the errors propagate. Fig. 3 shows the foot stamps of the two feet while in motion.

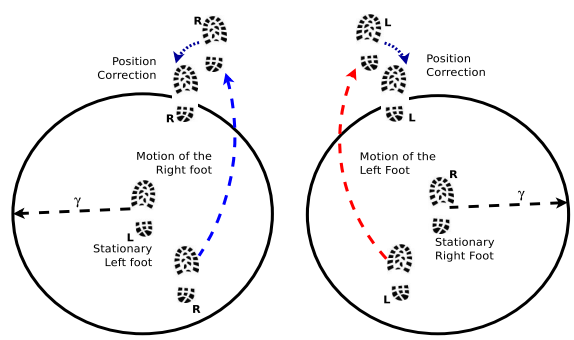

(a) Right foot position estimates after correction.

(b) Left foot position estimates after correction.

Figure 3: Cross section of a sphere of radius γ, which is the maximum possible spatial separation between the two feet.

A. Proposed Algorithm

Let $d_k^j = norm([\hat{\mathbf{x}}_k^i]_{1:3} - [\hat{\mathbf{x}}_k^j]_{1:3})$ represent the separation between the two navigation systems $i, j \in \{l, r\}$ and $i \neq j$, at any given instance of time k. If the ith navigation systems

is in stance phase (ZuPT is ON), the jth navigation system is not in stance phase and the separation between them is $d_k^j > \gamma$, then the new position coordinates of the jth navigation system is obtained as follows

$$\hat{\mathbf{p}}_k^j = \frac{1}{d_k^i}\left((d_k^i - \gamma)[\hat{\mathbf{x}}_k^i]_{1:3} + \gamma[\hat{\mathbf{x}}_k^j]_{1:3}\right). \quad (10)$$

We define an observation matrix $\mathbf{H'}_k^i$ for the ith navigation system where $i \in \{l, r\}$ as follows

$$\mathbf{H'}_k^i = \begin{bmatrix}\mathbf{I}_3 & \mathbf{0}_3 & \mathbf{0}_3\end{bmatrix}. \quad (11)$$

The process noise $\mathbf{w}_k^{3i} \in \mathbb{R}^3$ is assumed to be white and the covariance matrix is defined as

$$\mathbf{R'}_k^i = \mathbb{E}\{\mathbf{w}_k^{3i}(\mathbf{w}_k^{3i})^T\} \quad (12)$$
$$= \sigma_p^2 \mathbf{I}_3 \quad (13)$$

Here $\sigma_p^2 \in \mathbb{R}^1$ denotes the variance of measurement noise. After the position estimates are corrected using equation (10), the estimates are updated incorporating the observation.

Algorithm 2 Pseudo code for the algorithm *with* a range constraint, γ on the spatial separation between the two navigation system i, j where $i, j \in \{l, r\}$ and $i \neq j$.

$k \leftarrow 0$
$\mathbf{P}_k^i, \mathbf{Q}_k^i, \mathbf{R}_k^i, \mathbf{H}_k^i, \mathbf{H'}_k^i \leftarrow$ **Process**{Initialize Filter}
$\mathbf{P}_k^j, \mathbf{Q}_k^j, \mathbf{R}_k^j, \mathbf{H}_k^j, \mathbf{H'}_k^j \leftarrow$ **Process**{Initialize Filter}
$\hat{\mathbf{x}}_k^i \leftarrow$ **Process**{Initial Navigation State}
$\hat{\mathbf{x}}_k^j \leftarrow$ **Process**{Initial Navigation State}
loop
  $k \leftarrow k + 1$
  $\hat{\mathbf{x}}_k^i \leftarrow$ **Process**{Navigation Equations}
  $\hat{\mathbf{x}}_k^j \leftarrow$ **Process**{Navigation Equations}
  $\mathbf{P}_k^i \leftarrow \mathbf{F}_k^i \mathbf{P}_{k-1}^i {\mathbf{F}_k^i}^T + \mathbf{G}_k^i \mathbf{Q}_k^i {\mathbf{G}_k^i}^T$
  $\mathbf{P}_k^j \leftarrow \mathbf{F}_k^j \mathbf{P}_{k-1}^j {\mathbf{F}_k^j}^T + \mathbf{G}_k^j \mathbf{Q}_k^j {\mathbf{G}_k^j}^T$
  for $i, j \in \{l, r\}$ and $i \neq j$ **do**
    if $\mathbf{zupt}_k^i$ is **on then**
      $\mathbf{K}_k^i \leftarrow \mathbf{P}_k^i {\mathbf{H}_k^i}^T [\mathbf{H}_k^i \mathbf{P}_k^i {\mathbf{H}_k^i}^T + \mathbf{R}_k^i]^{-1}$
      $\delta\mathbf{x}_k^i \leftarrow -\mathbf{K}_k^i [\hat{\mathbf{x}}_k^i]_{4:6}$
      $\hat{\mathbf{x}}_k^i \leftarrow$ **Process**{Correct Nav. States}
      $\mathbf{P}_k^i \leftarrow [\mathbf{I} - \mathbf{K}_k^i \mathbf{H}_k^i]\mathbf{P}_k^i$
      if $\mathbf{zupt}_k^j$ is **off** and $d_k^j > \gamma$ **then**
        $\hat{\mathbf{p}}_k^j \leftarrow$ **Process**{Correct Position}
        $\mathbf{K'}_k^j \leftarrow \mathbf{P}_k^j \mathbf{H'}_k^j {\mathbf{H'}_k^j}^T [\mathbf{H'}_k^j \mathbf{P}_k^j {\mathbf{K'}_k^j}^T + \mathbf{R'}_k^j]^{-1}$
        $\delta\mathbf{x}_k^j \leftarrow \mathbf{K'}_k^j (\hat{\mathbf{p}}_k^j - [\hat{\mathbf{x}}_k^j]_{1:3})$
        $\hat{\mathbf{x}}_k^j \leftarrow$ **Process**{Correct Nav. States}
        $\mathbf{P}_k^j \leftarrow [\mathbf{I} - \mathbf{K'}_k^j \mathbf{H'}_k^j]\mathbf{P}_k^j$
      end if
    end if
  end for
end loop

IV. Experiment and Results

From the results presented in Fig. 5, we can observe that except for the straight path trajectory, all the other trajectories have diverged from the actual path. Even though the left and right trajectories are in sync, they don't represent the actual path information. In all the trajectories shown in Fig. 5, we assumed an initial heading of $0°$ for left and right navigation system. In Fig. 6, we tune this initial heading value and run the proposed algorithm. The trajectories obtained and the actual path are almost the same except for the inverted 'U' path trajectory where we see the end points not being the same. Comparing the results obtained in Fig. 4, Fig. 5 and Fig. 6, we observe that the proposed algorithm with initial heading estimates gives the best trajectory information which is closely similar in shape to the actual trajectory.

To test the performance of the proposed algorithm with the existing algorithm in [4], we make use of the same data sets that were used in [4]. A user equipped with one OpenShoe on each foot, walked 110 meters on level ground along a straight line at a normal gait speed. A total of 40 datasets were collected, using two different sets of OpenShoe units. The authors in [4] use constrained least square optimization to reduce the systematic heading drift. Refer to www.openshoe.org for details about the OpenShoe navigation system and for downloading the data sets. The code for [4] is also available in the same website. We have modified the code and made changes to incorporate our proposed algorithm and compared the scatter plot results of existing and proposed algorithms in Fig. 7. It is clearly seen that the mean and covariance of final position estimates are significantly reduced by applying the range constraint and the results are comparable with the existing algorithm.

V. Conclusions

The proposed method to fuse information from two navigation systems uses a Kalman filter in order to reduce the systematic heading drift. The two navigation systems are connected with an upper bound on their spatial separation. The proposed algorithm is easy to implement and also the computation complexity is low as it involves matrix multiplications and computing inverse of a 3×3 matrix. The proposed algorithm performs more efficiently when the initial heading estimates are known.

Acknowledgments

This project is jointly funded by Department of Science and Technology, Govt. of India and VINNOVA, Sweden. We would also like to thank Isaac Skog and John Nilsson for making the data sets and code readily available at www.openshoe.org.

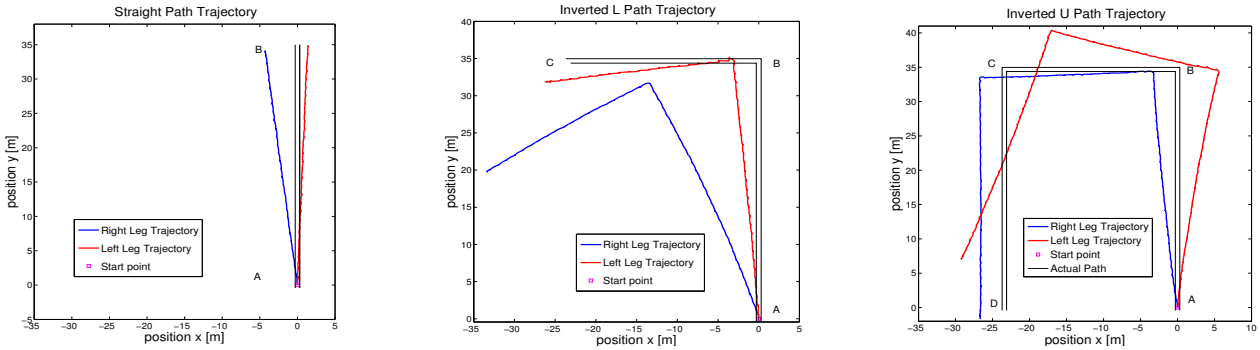

(a) Left and Right foot trajectory for Straight Path along segment AB.

(b) Left and Right foot trajectory for Inverted 'L' Path along segment AB and BC.

(c) Left and Right foot trajectory for Inverted 'U' Path along segment AB, BC and CD

Figure 4: Trajectories obtained after applying the algorithm without any range constraint on the spatial separation between two feet. Initial heading value is equal to 0° for all data sets.

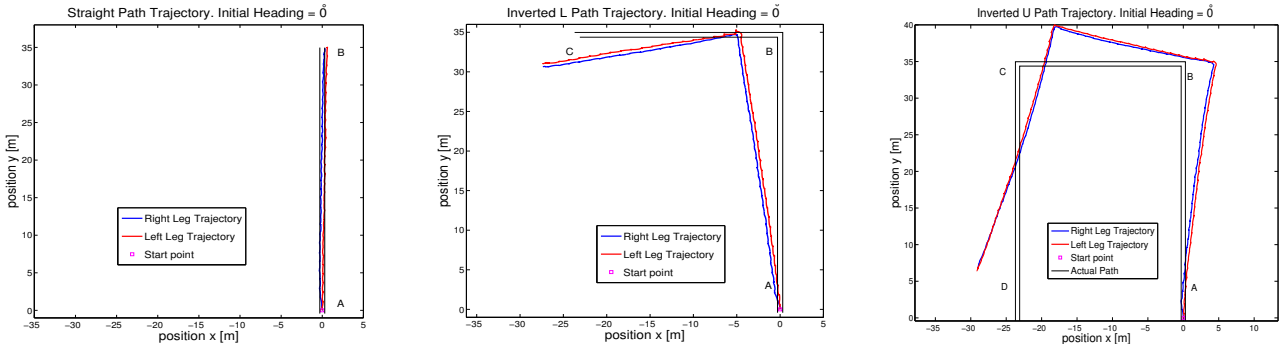

(a) Left and Right foot trajectory for Straight Path along segment AB using proposed algorithm.

(b) Left and Right foot trajectory for Inverted 'L' Path along segment AB and BC using proposed algorithm.

(c) Left and Right foot trajectory for Inverted 'U' Path along segment AB, BC and CD using proposed algorithm

Figure 5: Trajectories obtained after applying the proposed algorithm with initial heading value equal to 0°. $\gamma = 0.6096$[m] for all the above trajectories.

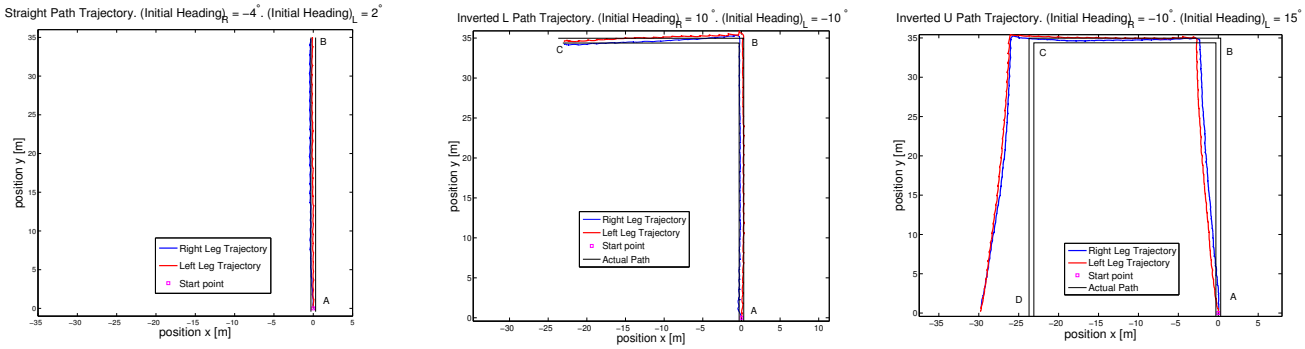

(a) Left and Right foot trajectory for Straight Path along segment AB using proposed algorithm with initial heading for right equal to -4° and initial heading for left equal to 2°.

(b) Left and Right foot trajectory for Inverted 'L' Path along segment AB and BC using proposed algorithm with initial heading for left equal to -10° and initial heading for right equal to 10°.

(c) Left and Right foot trajectory for Inverted 'U' Path along segment AB, BC and CD using proposed algorithm with initial heading for right equal to -10° and initial heading for left equal to 15°.

Figure 6: Trajectories obtained after applying the proposed algorithm with an estimate of initial heading value available before hand. The trajectories obtained and the actual trajectories almost match. $\gamma = 0.6096$[m] for all the above trajectories.

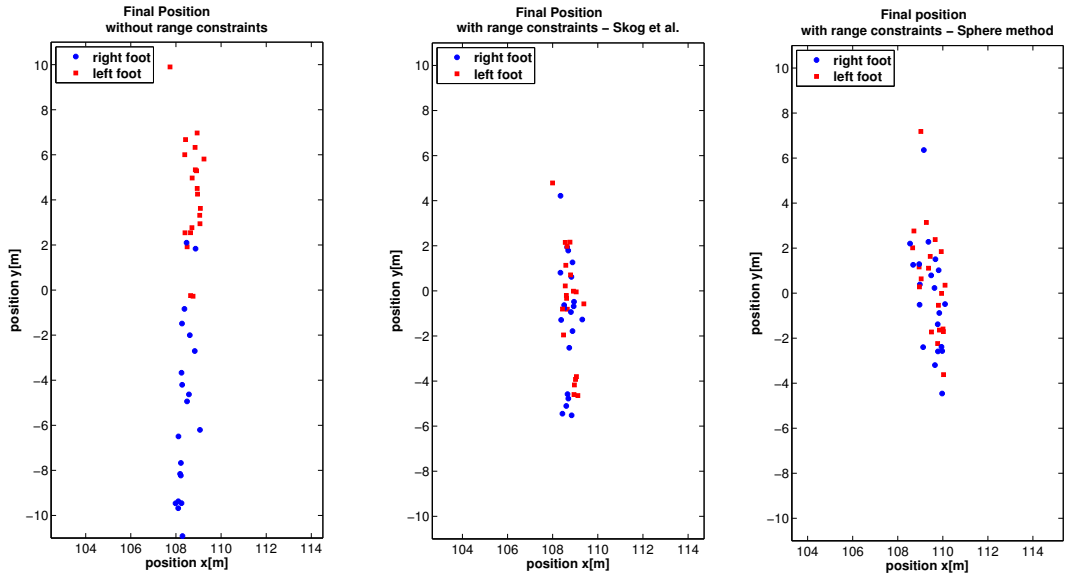

Figure 7: Scatter plot of end position of the two systems *with* and *without* range constraint for existing [4] and proposed algorithm from walking along a 110[m] straight line. The scatter plots obtained are for $\gamma = 1$[m] for all the datasets for the existing and proposed algorithm. The heading estimate is obtained at 10[m].

References

[1] J. Rantakokko, J. Rydell, P. Stromback, P. Handel, J. Callmer, D. Tornqvist, F. Gustafsson, M. Jobs, and M. Gruden, "Accurate and reliable soldier and first responder indoor positioning: multisensor systems and cooperative localization," *Wireless Communications, IEEE*, vol. 18, pp. 10 –18, april 2011.

[2] I. Skog, J.-O. Nilsson, P. Handel and K.V.S. Hari , "Foot-mounted INS for everybody - an open-source embedded implementation," *Position Location and Navigation Symposium (PLANS), 2012 IEEE/ION* , vol., no., pp.140-145, 23-26 April 2012 doi: 10.1109/PLANS.2012.6236875

[3] J.-O. Nilsson, I. Skog and P. Handel, "A note on the limitations of zupts and the implications on sensor error modeling," to appear in *Indoor Positioning and Indoor Navigation (IPIN)* dec 2012.

[4] I. Skog, J.-O. Nilsson and P. Handel, "Fusing the information from two navigation systems using an upper bound on their maximum spatial separation," to appear in *Indoor Positioning and Indoor Navigation (IPIN)* dec 2012.

[5] J. B. Bancroft, G. Lachapelle, M. E. Cannon and M. G. Petovello, "Twin IMU-HGPS integration for pedestrian navigation," in *Proc. ION GNSS*, 2008.

[6] T. Brand and R. Phillips, "Foot-to-foot range measurement as an aid to personal navigation," in Proc. *59th Annual Meeting of The Institute of Navigation and CIGTF 22nd Guidance Test Symposium*, 2003.

[7] D. Zachariah, I. Skog, M. Jansson, and P. Handel, "Bayesian estimation with distance bounds," *Signal Processing Letters, IEEE*, vol. 19, pp. 880 –883, dec. 2012.

[8] I. Skog, J.-O. Nilsson and P. Handel, "Evaluation of zero-velocity detectors for foot-mounted inertial navigation systems," in *Indoor Positioning and Indoor Navigation (IPIN), 2010 International Conference on*, pp. 1 –6, sept. 2010.

[9] I. Skog, P. Handel, J. Nilsson, and J. Rantakokko, "Zero-velocity detection - an algorithm evaluation," *Biomedical Engineering, IEEE Transactions on*, vol. 57, pp. 2657 –2666, nov. 2010.

[10] Kwakkel, S.P., Lachapelle, G., Cannon, M.E., "GNSS Aided In Situ Human Lower Limb Kinematics During Running," *Proceedings of the 21st International Technical Meeting of the Satellite Division of The Institute of Navigation (ION GNSS 2008)*, Savannah, GA, September 2008, pp. 1388-1397.

[11] J. A. Farrell and M. Barth, "The Global Positioning System and Inertial Navigation". *McGraw-Hill, 1998.*